Supporting Information

A Novel Capillary Microplasma Analytical System: Interface-free Coupling of Glow Discharge Optical Emission Spectrometry to Capillary Electrophoresis

Xue Jiang[a], Xinliang Xu[b], Xiandeng Hou[a,c], Zhou Long[c], Yunfei Tian[c], Xiaoming Jiang[c], Fujian Xu[c], and Chengbin Zheng[a*]*

[a] Key Laboratory of Green Chemistry & Technology, Ministry of Education, College of Chemistry, Sichuan University, Chengdu, Sichuan 610064, China

[b] York Plasma Institute, University of York, York, NorthYorkshire, YO10 5DD, UK

[c] Analytical & Testing Center, Sichuan University, Chengdu, Sichuan 610064, China. & Testing Center, Sichuan University, Chengdu, Sichuan 610064, China

*Corresponding authors:

E-mails: houxd@scu.edu.cn (Hou XD) and abinscu@scu.edu.cn (Zheng CB)

Table of Content

1. Reverse C-µPAS.

The reverse C-µPAS was constructed by exchanging the cathode and the anode. The tungsten electrode as the anode and the capillary liquid electrode as the cathode. Therefore, anions could be separated and detected in the microplasma by the C-µPAS.

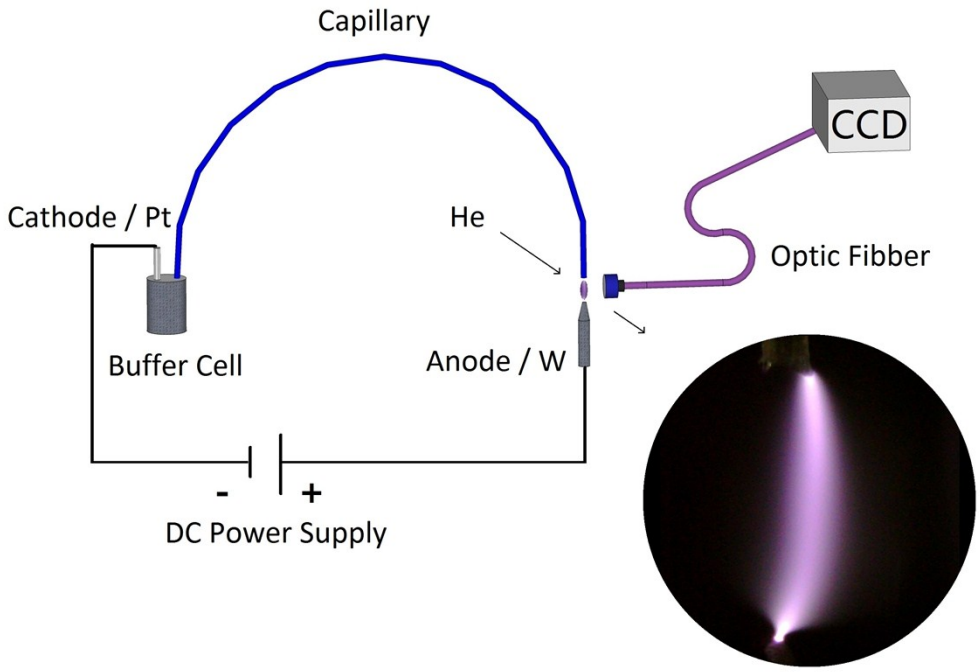

Fig. S1 A schematic of the reverse C-µPAS. The insert is the photo of the bright microplasma.

2. Operation conditions of HPLC-ICP-MS.

Table S1. The operation parameters of HPLC-ICP-MS

Parameters	**values**
HPLC	Thermo U3000
Column	Thermo Syncronis Sillca (150 ×4.6×5 μm)
Mobile phase	Methanol
Flow rate of the mobile phase (L/min)	0.001
Injection volume (μL)	20
ICP-MS	Thermo iCAPQ
RF(W)	1550
Flow rate of nebulizer gas (L/min)	1.0
Flow rate of auxiliary gas (L/min)	0.5
Flow rate of plasma gas (L/min)	13
Quantification	Peak area

3. Relationship between current and voltage of C-µPAS and reverse C-µPAS.

Table S2. The relationship of the current and the voltage of the proposed setup.

	Voltage / kV	**Current / mA**
C-µPAS (Ar)	1.0	0.01
	2.0	0.03
	3.0	0.07
	4.0	0.10
	5.0	0.16
	6.0	0.22
	7.0	0.27
Reverse C-µPAS (He)	1.0	0.01
	2.0	0.04
	3.0	0.07
	4.0	0.09
	5.0	0.13
	6.0	0.21
	7.0	0.25

4. Optimization of voltage of C-µPAS for separation.

In this work, the voltages from 2.0 kV to 4.0 kV were tested for mercury detection to investigate the effect of voltage on the separation of C-µPAS. A lower voltage took longer time to observe the apperance of the signal, because the current was lower and the migration rate of mobile ions.

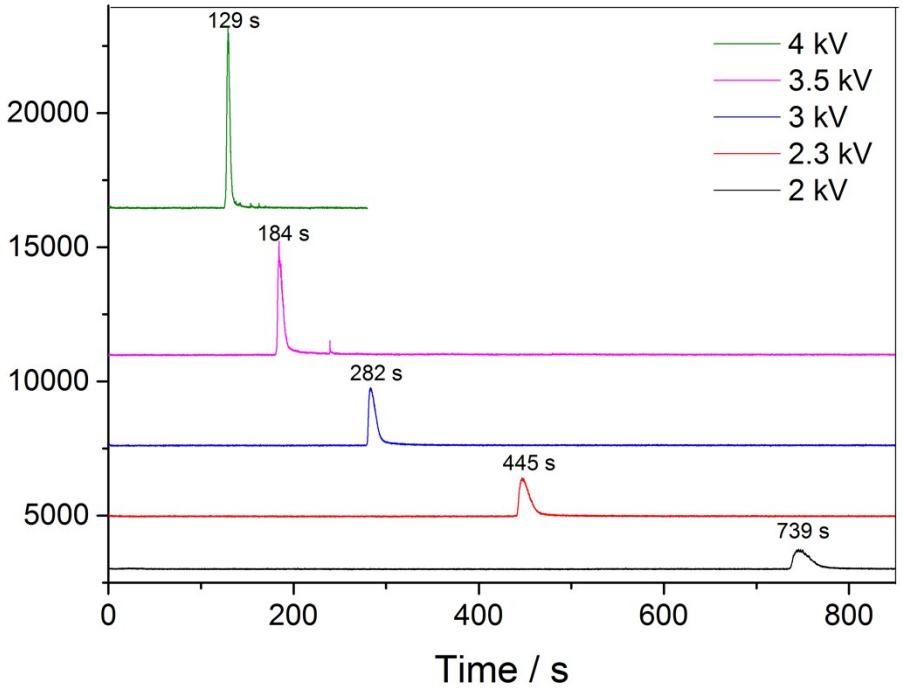

Fig. S2 The effect of voltage on the separation of C-µPAS. Working conditions: sample: 100 µg/ L Hg^{2+}; working voltage: 2.0 kV-4.0 kV; current: 30 µA-100 µA; discharge area: 3.0×1.0 mm^2; and the flow rate of Ar: 200 mL/min.

5. Optimization of injection time of C-μPAS for separation.

With the gravity injection method, it seemed no obvious difference between the injection time from 0.1 s to 10 s in the retention time.

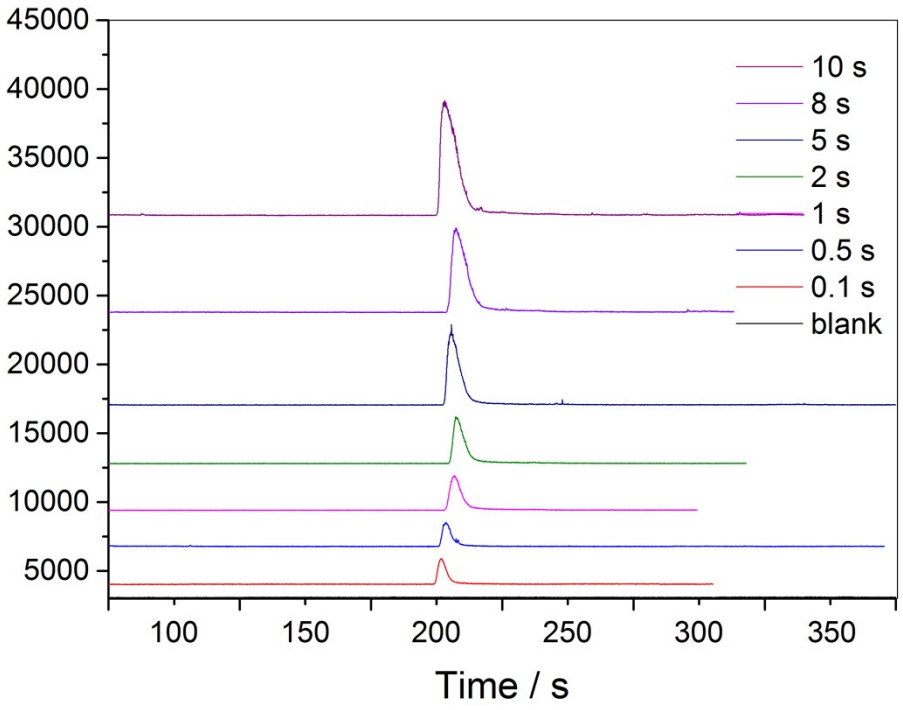

Fig. S3 The effect of the injection time on the separation of C-μPAS.
Working conditions: sample: 100 μg/L Hg^{2+}; working voltage: 3.0 kV; current: 70 μA; discharge area: 3.0×1.0 mm^2; and the flow rate of Ar: 200 mL/min.

6. Atomic emission spectra for several elements in C-μPAS.

Compared with a blank, Hg atomic emission line (253.7 nm), Cd atomic emission lines (228.8 nm), Ca atomic emission line (458.6 nm), Cr atomic emission line (267.7 nm) and Na atomic emission line (589.0 nm) were clearly identified in the optical emission spectrum.

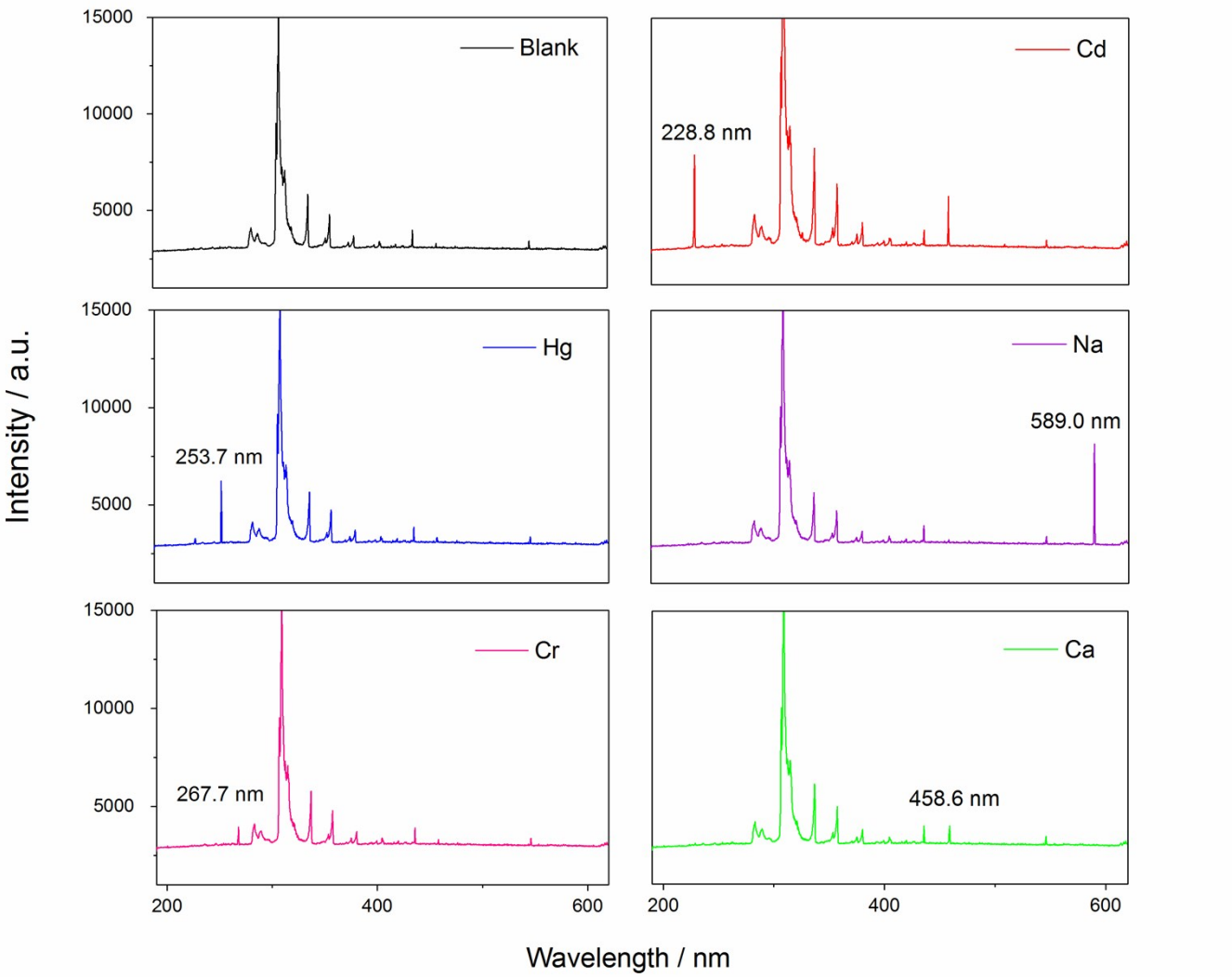

Fig. S4 Optical emission spectrum of Hg atomic emission line (253.7 nm), Cd (228.8 nm), Ca (458.6 nm), Cr (267.7 nm) and Na (589.0 nm) in the C-μPAS. Working conditions: sample: 100 μg/L analytes; working voltage: 3.0 kV; current: 70 μA; discharge area: 3.0×1.0 mm^2; injection time: 5 s; and the flow rate of Ar: 200 mL/min.

7. Calculation of electron temperature and electron density of microplasma.

The OH rotational temperatures were calculated based on the rotational fine structure of the ($A^2\Sigma+\rightarrow X^2\Pi_i$) OH band at 306.4 nm, 308.6 nm and 311.8 nm by means of a Boltzmann plot.

$$\frac{n_n}{n_m} = \frac{g_n}{g_m}\exp[-\frac{E_n - E_m}{kT}]$$

Firstly, the number of the electrons obeys the relationship with their energy level E_n and E_m, and the E_n-E_m is related to the spectral frequency. By using Log function on both sides, the equation can be rewritten as:

$$\ln(\frac{n_n}{g_n}) = -\frac{1}{kT}E_n + D$$

Where D is a constant. By using the method linear regression, the electron temperature of the microplasma was obtained (Fig. 5a).

In addition, combined with the temperature, it is not hard to figure out the Stark broadening of the spectrum.

$$\Delta\lambda_{stark} = 2\times\left[1 + 1.75\times10^{-4}\times\sqrt[4]{N_e}\alpha\times(1 - 0.068\sqrt[6]{N_e}\frac{1}{\sqrt[2]{T_e}})\right]\times10^{-16}\omega N_e$$

Where α is the static ion-broadening parameter, ω is electron impact half-width. $\Delta\lambda_{Stark}$ is a function of T_e and N_e (the electron density), α and ω are both function of T_e. After the $\Delta\lambda_{Stark}$ measured, the electron density of the microplasma was obtained.

8. Background emission from discharge gas in C-μPAS.

In this work, three different gases, including Air, Ar and He, were tested as the discharge gas to investigate the background emission of the carrier gas on the spectral response.

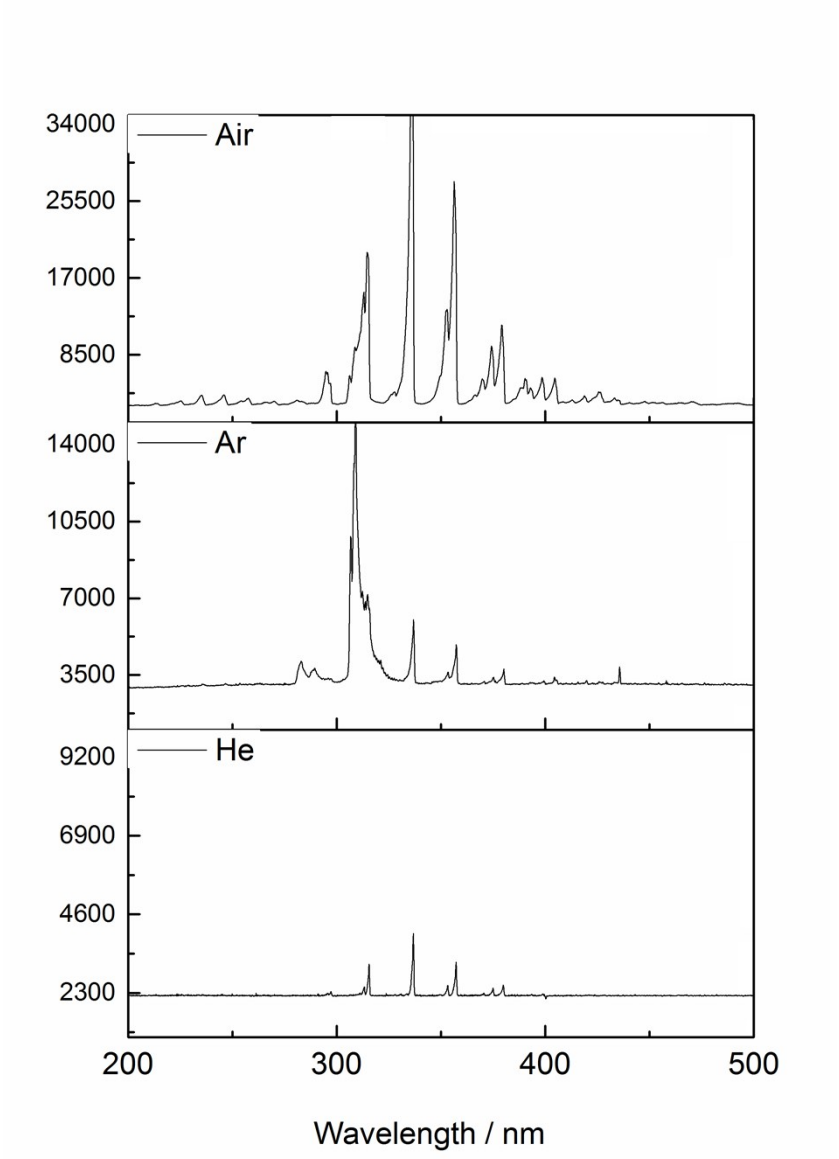

Fig. S5 The effect of the discharge gas type on the background emission spectra. Working conditions: working voltage: 3.0 kV; current: 70 μA; discharge area: 3.0×1.0 mm^2; and the flow rate of Ar/Air/He: 200 mL/min.

9. Effect of Ar flow rate on mercury atomic emission.

The spectral responses of mercury atomic emission significantly changed with the flow rate of Ar throughout the range of 50 - 600 mL/min in the C-μPAS.

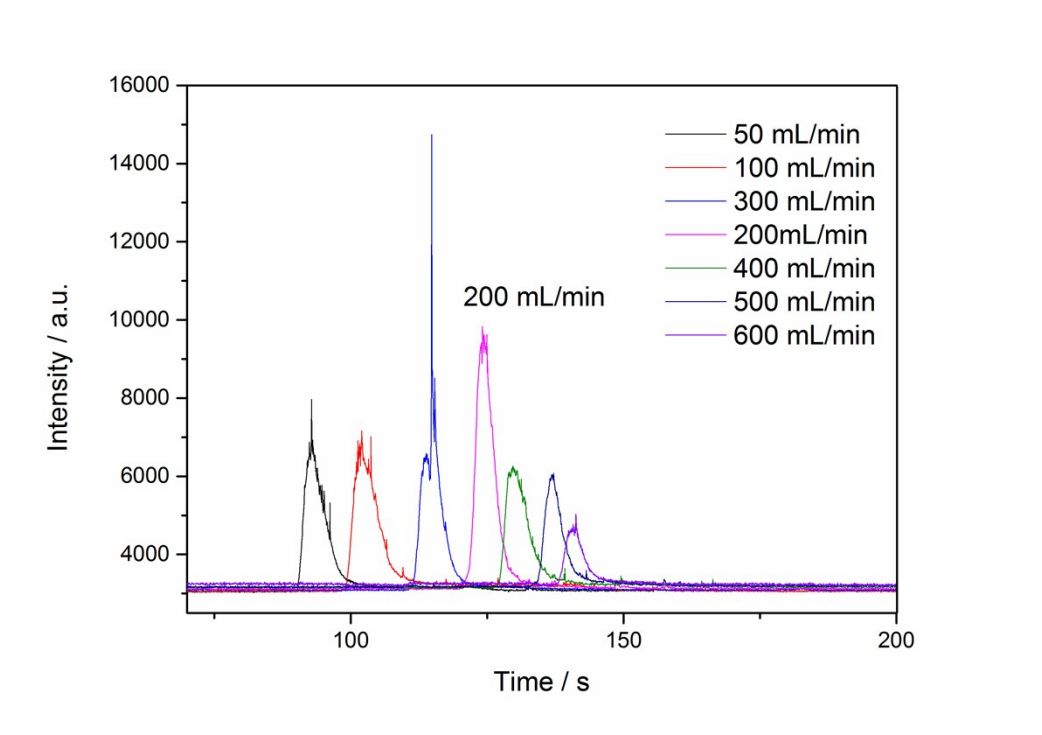

Fig. S6 Effect of flow rate of discharge gas on the mercury atomic emission signal. Working conditions: working voltage: 3.0 kV; current: 70 μA; discharge area: 3.0×1.0 mm^2; and Hg^{2+} concentration: 100 μg/L.

10. Influence of analyte concentration.

In the initial experiments, 0.1 μg/mL and 10 μg/mL of Hg atomic emssion spectra were tested. High concentration led to problematic tailing.

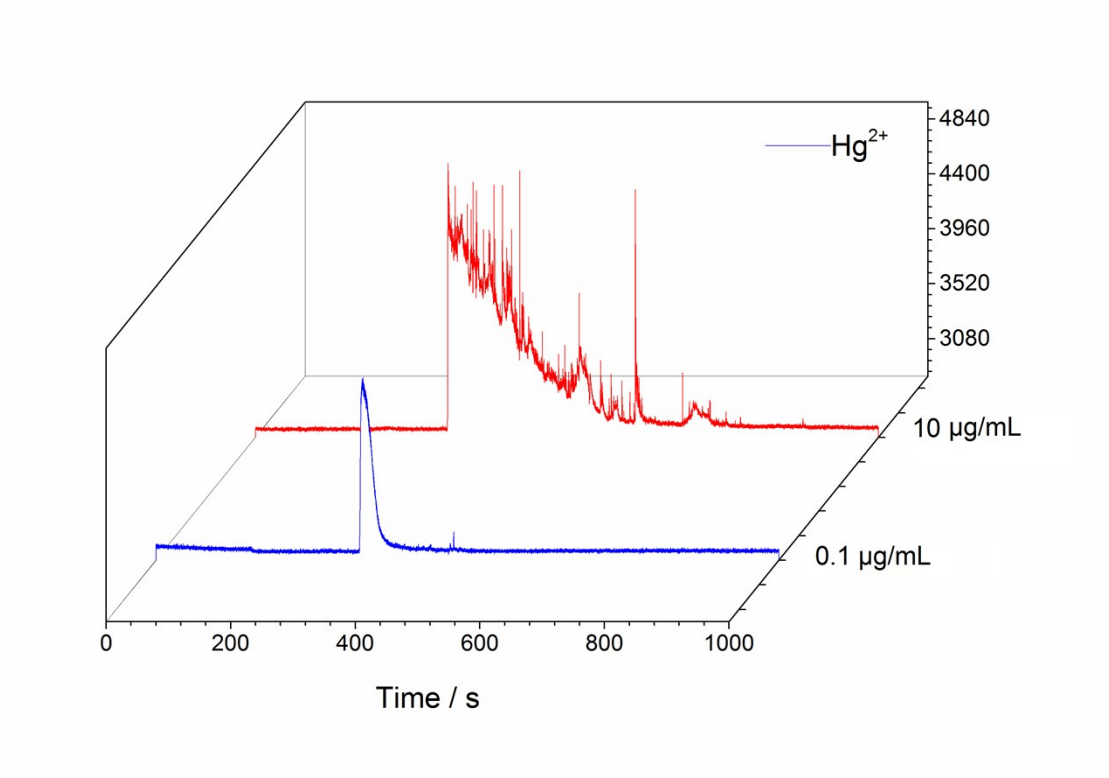

Fig. S7 Effect of mercury concentration on the atomic emission spectra. Working conditions: working voltage: 3.0 kV; current: 70 μA; discharge area: 3.0×1.0 mm^2; and the flow rate of Ar: 200 mL/min.

11. Comparison of LODs for metals by this method with those reported in references.

Table S3. Comparison of the LODs by this method with those reported in references

Method	RSD (%)	LOD (μg/L)	Derivatization	Operation	Interface	Reference
CE-UV	<10	13-509	Yes	Easy	No	[1]
CE-CD	<5	5-30 nmol/L	Yes	Easy	No	[2]
CE-EC	<5	5-40 nmol/L	No	Complex	No	[3]
CE-FL	<8	0.1-0.3 μmol/L	Yes	Easy	Yes	[4]
CE-ICP-OES	<3	0.3-6	No	Easy	Yes	[5]
CE-MIP-OES	<7	3.9-5.4	Yes	Complex	Yes	[6]
CE-ICP-MS	<5;	0.021-0.032	Yes	Complex	Yes	[7]
	<6	0.9 -3.0	No			[8]
μ-PAS	<5	2-40	No	Easy	No	This work

12. Photo of C-μPAS.

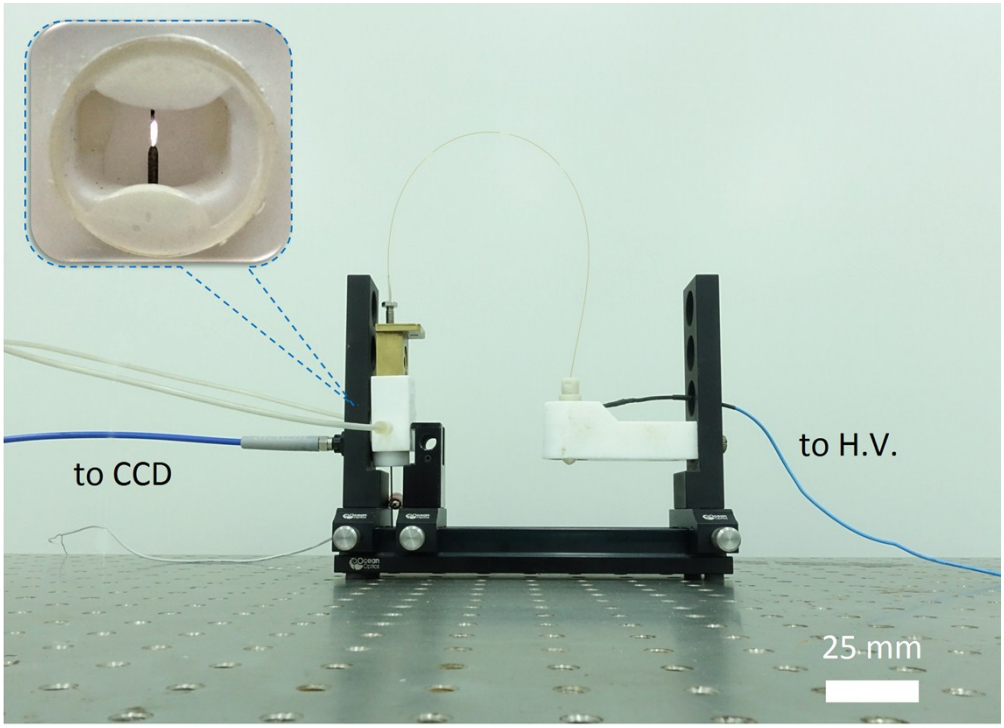

Fig. S8 The photo of our C-μPAS.

Reference:

[1] C. Casiot, M. Carmen Barciela Alonso, O. F. X. Donard, M. Potin-Gautier, M. Carmen Barciela Alonso, J. Boisson, *Analyst* , 1998, **123**, 2887.

[2] F. Tan, B. Yang, Y. Guan, *Analytical Sciences*, 2005, **21,** 955.

[3] J. Wen, A. Baranski, R. Cassidy, *Analytical Chemistry,* 1998, **70**, 2504.

[4] R. Zhu, W.T. Kok, *Analytica Chimica Acta*, 1998, **371**, 269.

[5] J.W. Olesik, J.A. Kinzer, S.V. Olesik, *Analytical Chemistry*, 1995, **67**, 1.

[6] H. Matusiewicz, M. Ślachciński, *Microchemical Journal* , 2012, **102**, 61.

[7] Y. Zhao, J. Zheng, L. Fang, Q. Lin, Y. Wu, Z. Xue, F. Fu, *Talanta,* 2012, **89**, 280.

[8] L. Liu, B. He, Z. Yun, J. Sun, G. Jiang, *Journal of Chromatography A*, 2013, **227**, 1304.